Impacts of a nano-enabled pesticide formulation (nTiO2-coated carbendazim) and its constituents on the freshwater snail Lymnaea stagnalis & damselfly Ischnura elegans assessed via in-situ bioassays

Nederstigt, T.A.P.; Frische, R.K.M.; Ouwehand, J.; Vijver, M.G.

Ecotoxicology and Environmental Safety 303 (2025) 118809

Contents lists available at ScienceDirect

Ecotoxicology and Environmental Safety

journal homepage: www.elsevier.com/locate/ecoenv

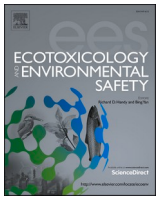

Impacts of a nano-enabled pesticide formulation ($nTiO_2$-coated carbendazim) and its constituents on the freshwater snail *Lymnaea stagnalis* & damselfly *Ischnura elegans* assessed via *in-situ* bioassays

Tom A.P. Nederstigt [*,†], Richard K.M. Frische [†], Jesse Ouwehand, Martina G. Vijver

Institute of Environmental Sciences (CML), Leiden University, Leiden, The Netherlands

ARTICLE INFO

Edited by Anita Jemec Kokalj

Keywords:
Controlled-release
Nanopesticide
Nanocarrier
Mesocosm
Invertebrate
Microbial community
Reactive oxygen species

ABSTRACT

Novel pesticidal products in which active substances are delivered via nanoscale carrier systems have been suggested to offer functional and environmental benefits over conventional pesticide formulations. Nevertheless, non-target impacts associated with such nano-enabled pesticides remain largely unexplored. The current study compares effects from a nano-TiO_2-coated formulation of carbendazim (i.e., $nTiO_2$-coated carbendazim) with those of its active substance (i.e., the fungicide carbendazim), coating material (i.e., nanoscale TiO_2), and a treatment in which the latter two are combined, by means of *in-situ* bioassays. Bioassays focused on the freshwater snail *Lymnaea stagnalis* and larvae of the damselfly *Ischnura elegans*, two invertebrate species representing different niches. For *L. stagnalis*, effects on survival, growth, and feeding were assessed over 29 days, and resource utilization rates of microbial communities present on its provided food source were analyzed to determine feeding-related indirect effects. For *I. elegans*, survival, feeding, emergence (i.e., development into imagines), and body size upon emergence were assessed over 57 days. Mortality rates of *L. stagnalis* increased by ~40 % in $nTiO_2$ and ~50 % in combined (i.e., carbendazim & $nTiO_2$) treatments applied at environmentally realistic concentrations, but insignificantly in $nTiO_2$-coated carbendazim treatments. We argue that differences in this regard are likely to have arisen from contrasting photocatalytic activity of the $nTiO_2$ utilized in respective treatments. Microbial community carbon utilization profiles exhibited minimal differences between treatments. *I. elegans* survival, feeding and growth rates were unaffected, but a slight decrease in emergence time was observed across treatments. The findings of the current study highlight that photocatalytic properties of nanomaterials can be an important factor for consideration regarding non-target impacts of nano-enabled products with agricultural applications.

1. Introduction

Freshwater ecosystems and the diversity of life which they host are vital in their functions to both the natural environment and human well-being (Hitt et al., 2015; Dudley et al., 2017; Reid et al., 2019). Numerous manmade substances and materials are however intentionally and unintentionally introduced into these systems, and current and emerging contaminants remain a key threat to freshwater biodiversity globally (Schwarzenbach et al., 2006; Haase et al., 2023). The growing application of engineered nanomaterials (ENMs), or nanoforms, in consumer products and industrial processes has received increasing attention to this end (Adam et al., 2021; Hendricks et al., 2023; Keller et al., 2023). While on the one hand constituting potential novel environmental contaminants themselves, ENMs may also offer opportunities to curb emissions of conventional substances. In this regard, the development of nano-enabled pesticide formulations has been suggested to represent a viable path towards reducing the displacement of pesticides to off-target ecosystems, and mitigating their impacts on non-target organisms (Koli et al., 2015; Kumar et al., 2017; Hofmann et al., 2020; Wang et al., 2022; Kah et al., 2023). Functionalities proposed to facilitate such reductions often rely on the encapsulation or binding of active substances to nanoscale carrier systems, aiming to extend their stability and activity under field conditions, and to provide time- and stimuli-dependent control over their delivery to crops or pest organisms. This in turn

* Corresponding author.
E-mail address: t.a.p.nederstigt@cml.leidenuniv.nl (T.A.P. Nederstigt).
† These authors contributed equally.

https://doi.org/10.1016/j.ecoenv.2025.118809
Received 21 February 2025; Received in revised form 23 July 2025; Accepted 2 August 2025
Available online 7 August 2025

could aid in lowering the volume of active substances required for effective pest control, reduce their displacement towards off-target sites, and thereby ultimately mitigate non-target impacts (Hayles et al., 2017; Grillo et al., 2021; Wang et al., 2022). Although functionalities such as these have frequently been suggested to offer real-world benefits of nano-enabled pesticide formulations, they have also been noted to exhibit potential to exacerbate non-target impacts of active substances by altering their fate, exposure dynamics, and bioavailability (Kookana et al., 2014; Nederstigt et al., 2024). In this regard, experimental studies that provide comparative estimates of impacts of nano-enabled pesticide formulations on non-target organisms (i.e., relative to their non-nanoscale analogs) have been sparse to date (Wang et al., 2022; Zhang and Goss, 2022; Nederstigt et al., 2024).

In addition to widely documented impacts resulting from their direct toxicity (Wan et al., 2025), displacement of pesticides towards freshwaters may affect non-target organisms indirectly via effects on ecologically-linked organisms and their related functional processes (Fleeger et al., 2003; Schäfer et al., 2011; Sánchez-Bayo and Ortiz-Santaliestra, 2021). The breakdown of organic matter, for example, constitutes a key step in nutrient cycling in freshwater ecosystems, and is mediated through an interplay of conditioning (i.e., partial enzymatic degradation) of detritus by fungi and bacteria, and its fragmentation and consumption by macroinvertebrate detritivores (Gessner et al., 1999; Graça, 2001; Hieber and Gessner, 2002). Previous studies have demonstrated that both ENMs and pesticides can adversely affect growth rates and survival of macroinvertebrates by impairing microbial conditioning of detritus, and that this can affect overall organic matter processing in streams (Zubrod et al., 2011; Flores et al., 2014; Zhai et al., 2018; Mohan et al., 2024). The presence of contaminants in freshwaters may also have reverberating impacts on adjacent terrestrial ecosystems. To this end, the developmental impairment of insects which exhibit aquatic juvenile- and terrestrial-flying adult life stages has received growing attention due to their importance in riparian food webs (Barmentlo et al., 2019; Pietz et al., 2023; Schulz et al., 2024). While indirect effects such as these may account for a considerable fraction of the overall environmental impacts of contaminants (including those in adjacent ecosystems), the design of commonly applied laboratory-based toxicity tests generally does not allow for their assessment (Fleeger et al., 2003; Barmentlo et al., 2019; Sánchez-Bayo and Ortiz-Santaliestra, 2021).

The current study provides a comparative assessment of direct and indirect effects of a novel nano-TiO_2-coated formulation of the fungicide carbendazim (i.e., nTiO_2-coated carbendazim), its constituents (i.e., carbendazim & nTiO_2), and a combined treatment of the latter two on two non-target freshwater invertebrates. *In-situ* bioassays were performed as part of a long-term outdoor mesocosm experiment, focusing on juveniles of the freshwater snail *Lymnaea stagnalis* and larvae of the damselfly *Ischnura elegans*. Both species are ubiquitous in freshwater ecosystems and exhibit a broad geographical distribution. *L. stagnalis* has previously been shown to play a substantial role in aquatic litter decomposition in littoral zones through grazing on (decaying) organic material (Schaller and Brackhage, 2015). *I. elegans* larvae are polyphagous predators, feeding predominantly on small invertebrates and zooplankton (Thompson, 1978). Treatment concentrations reflected those detected in surface waters for both the active substance (i.e., carbendazim) and the coating material (i.e., nTiO_2). Mortality rates and life history traits (growth in weight and length, food consumption) of *L. stagnalis* were assessed over 29 days. In addition, resource utilization rates and functional diversity of microbial communities on the food source provided to *L. stagnalis* was analyzed through use of Biolog™ ECO-plates, and periphyton growth (a potential secondary food source) was assessed in the test system. Finally, survival, the time until emergence, and body size upon emergence (i.e., as imagines) of *I. elegans* larvae, and their predation on *Chironomus sp.* larvae were recorded over 57 days.

2. Methods

2.1. Experimental setup

The experiment consisted of *in-situ* bioassays performed in an outdoor mesocosm test system designed to mimic agricultural ditches. This test system is part of the 'Living Lab' research facility located in Oegstgeest-Leiden, the Netherlands (see http://mesocosm.org/ for an extensive description of the experimental site). Ecological communities in each mesocosm (used length-width-depth: 5–0.8–0.3 m; volume: 1200 L) were established naturally via land, air and an adjacent pond over a period of three months (January 2020 - March 2020) prior to the start of the experiment. Mesocosms were subsequently hydrologically disconnected from the pond and allowed to settle for an additional month. Results from measurements of abiotic parameters and a detailed description of the synthesis, characterization, application, and analysis of all treatments in the experimental setup have been reported previously in Nederstigt et al. (2022).

2.2. Treatments

The experimental design consisted of a nano-TiO_2-coated controlled-release product of carbendazim (nTiO_2-coated carbendazim) and its constituents applied separately (nTiO_2, carbendazim) and in combination (carbendazim & nTiO_2) over seven replicate mesocosms per treatment. nTiO_2-coated carbendazim was custom-synthesized for the purpose of the experiment using pulsed chemical vapor deposition (pCVD). The applied pCVD process resulted in a nanoscale layer of amorphous TiO_2 being deposited onto dry carbendazim powder, which served as a diffusion barrier via which the release of carbendazim to its surrounding environment was extended over time.

The nTiO_2 used for the experiment consisted of a mixture of ~85 % anatase: ~15 % rutile crystalline structures with pristine particle sizes of 15–24 nm (JRCNM01005a, European Commission – DG JRC, also provided by Degussa/Evonik as AEROXIDE P25®). Nominal starting concentrations of nTiO_2 were 20 μg L^{-1}, which is within the range of reported concentrations (0.2–450 μg L^{-1}) of anthropogenically-derived TiO_2 in European and North American surface waters (Peters et al., 2018; Nabi et al., 2022). Carbendazim (CAS Number 10605–21–7, Sigma Aldrich, Missouri, USA) was applied in a single application at nominal treatment concentrations of 4 μg L^{-1}, with the aim of achieving time-weighted-average (TWA) concentrations of ~0.6 μg L^{-1} throughout the experiment, resembling measured surface water concentrations globally (Merel et al., 2018; Wan et al., 2021; Alejandro et al., 2022). In nTiO_2-coated carbendazim and carbendazim & nTiO_2 treatments, materials were applied at equivalent treatment concentrations as described for their individual constituents. Measured water column concentrations of all treatments in the experimental setup (from samples collected directly after treatment application, and one, two, seven, 14, 30, and 60 days thereafter), and release patterns of carbendazim from the nTiO_2-coated product have previously been reported and discussed in Nederstigt et al. (2022), and are summarized in SI Table 1.

Toxicity of nTiO_2 in the environment has been suggested to be partly attributable to its photocatalytic properties (Farner et al., 2019; Abdel-Latif et al., 2020; Coral et al., 2021), where irradiation with UV-A in aqueous media (i.e., upon irradiation with sunlight) results in the generation of reactive oxygen species (ROS), a process which is e.g., harnessed intentionally in antimicrobial applications (Gligorovski et al., 2015; Brinkmann et al., 2020). Amorphous crystalline structures of nTiO_2 (as present in the nTiO_2-coated carbendazim treatments) generally exhibit lower rates of ROS production than anatase and rutile structures (as present in the nTiO_2 and carbendazim & nTiO_2 treatments), and hydroxyl radicals (•OH) have been found to be the primary species generated through photocatalytic activity of nTiO_2 (Clément et al., 2013; Gligorovski et al., 2015; Farner et al., 2019). To aid in the

interpretation of potential differences in observed effects between treatments, relative •OH production rates of the $nTiO_2$ present on the coated carbendazim formulation and of the $nTiO_2$ applied in the $nTiO_2$ and carbendazim & $nTiO_2$ treatments were assessed following a method adapted from Farner et al. (2019). A 0.1 mM solution of terephthalic acid (TA, ≥ 98 %, Sigma-Aldrich, Missouri) in Elendt M7 medium (OECD, 2004) was loaded onto 96-well plates (200 μL per well total volume) containing either form of $nTiO_2$ (5 mg L^{-1}), in parallel to blanks containing only TA ($n = 5$ per treatment). Upon reaction with •OH, TA is converted to 2-hydroxyterephthalic acid, and fluorescence from the latter has been found to increase proportionally with the amount of generated •OH (Eremia et al., 2008). Plates were incubated in the dark and under irradiation with a UV-A source (F15W/T5/BL359; Sylvania, Amsterdam, The Netherlands), and analyzed for fluorescence intensity (excitation = 315 nm, emission = 425 nm) in a Tecan Infinite M1000 plate reader (Tecan, Männedorf, Switzerland) over three hours. Relative •OH production rates were determined as the difference in fluorescence intensity from mean blank values.

2.3. *Lymnaea stagnalis* - in-situ conditions and assessment of endpoints

L. stagnalis life history traits of survival, growth in size and weight, and feeding were assessed over 29 days in an *in-situ* caged setup. Approximately one-month-old *L. stagnalis* (175 in total) were randomly selected from an in-house culture with individuals originally derived from a culture maintained at Vrije Universiteit (Amsterdam, The Netherlands). *L. stagnalis* were subsequently conditioned for 15 days in water from the mesocosms at experimental site from which zooplankton was filtered out (filter mesh size ϴ 53 μm, EFE & GB Nets, Cornwall, UK), and divided into groups of five. Prior to the experiment, individuals were photographed from a fixed position (Iphone SE 2016, California, USA) including a reference scale, and shells (5.30 ± 0.06 mm, mean ± standard error) were measured in their greatest dimension, from the outermost edge of the opening to the apex using ImageJ ver. 1.53a (Schneider et al., 2012). In addition, wet weight for all individuals (11.02 ± 0.14 mg, mean ± SE) was determined after having been blotted onto absorbent paper to remove adhered water droplets. Each lot of five *L. stagnalis* was subsequently placed in a 400 mL polyethylene (PET) cage together with a previously weighed DECOTAB (see Section 2.4) as a food source, upon which cultured individuals were observed to feed readily. Cages were closed with a 0.5 mm polyester mesh and affixed upright to rods, with the opening of the cages facing upwards. On the day of treatment application, rods were placed in the center of the mesocosms, resulting in the cages being submerged halfway along the depth of the water column (see SI Figure 1 for an impression of the experimental setup). On days one, nine, 15 and 29 (after treatment application), cages were removed from the mesocosms and the number of surviving individuals was counted. After 29 days, shell length and wet weight of surviving individuals was measured again as described above. Growth in length and wet weight was calculated as the change in average values measured across all five individuals per replicate at the start of the experiment and the average values measured in individuals that survived until the end of the experiment (i.e., mean of survivors at end - mean value of all individuals at start).

2.4. *Lymnaea stagnalis* feeding substrate and microbial colonization - DECOTABs and fouling strips

Decomposition and consumption tablets (DECOTABs) were used as a food source to measure *L. stagnalis* feeding rates and to determine functional diversity parameters of microbial communities associated with organic matter (Kampfraath et al., 2012). To prepare DECOTABs, 20 g of agar was dissolved in 1 L heated demineralized water, followed by the addition of 60 g of < 250 μm-sized filaments of organic hay to the agar solution. Conditioning of DECOTABs took place over a period of 15 days in water collected from the mesocosms at the experimental site from which zooplankton was filtered out (filter mesh size ϴ 53 μm, EFE & GB Nets, Cornwall, UK). One DECOTAB was subsequently placed into each of the cages with *L. stagnalis*, and DECOTAB consumption by *L. stagnalis* was assessed by determining the wet weight of DECOTABs before insertion into cages and after the experiment, and normalized according to observed survival rates per measurement interval. Prior to weighing, DECOTABs were blotted on an absorbent paper towel to remove excess water adhering to the surface. Dry weights were obtained by converting wet weights using the average moisture content (5.89 ± 0.49 %, mean ± SE), determined from a subset of unused DECOTABs ($n = 4$) from the same production batch after drying at 60 °C for 72 h, after which no further change in weight was observed.

Periphyton was considered as a potential additional food source for *L. stagnalis* in the experimental setup, and periphyton development was therefore measured by placing six microscopy slides measuring ~76x26x1 mm upright in additional 400 mL PET cages in each mesocosm, acting as fouling strips. Prior to placement in the PET cages, microscopy slides were sandblasted to create a coarser surface and subsequently degreased and washed. At the end of the experiment two slides from each mesocosm were retrieved at random and freeze-dried in a Christ Alpha freeze dryer (Martin Christ GmbH, Osterode am Harz, Germany). The dried material was thoroughly scraped from all surfaces and weighed to measure overall accumulated dry biomass in μg/cm^2.

2.5. Functional composition of DECOTAB microbial communities - Biolog™ ECO-plates

The functional composition of DECOTAB-associated microbial communities was analyzed using Biolog™ ECO-plates (Biolog™, Hayward, California, USA). Biolog™ ECO-plates are 96-well plates which consist of three sets of 31 carbon substrates (grouped as seven carboxylic acids, four polymers, 10 carbohydrates, two phenolic compounds, six amino acids, and two amines) and a blank. Each well contains the redox dye tetrazolium violet, and utilization of a carbon substrate results in a colorimetric shift of the dye, thereby providing a quantitative measure of the extent to which the applied microbial community is able to utilize specific carbon substrates.

DECOTABs collected after 29 days from the *L. stagnalis* experiment ($n = 6$ per treatment) were placed in sterile 50 mL tubes, submerged to the 50 mL mark in demineralized water, and stored at 4 °C in the dark until use for inoculation of the Biolog™ ECO-plates. Tubes were shaken by hand and 100 μL of inoculate was distributed into each well on Biolog™ ECO-plates. Biolog™ ECO-plates were incubated at 28 °C and measured for optical density at 590 nm on a Tecan Infinite M1000 plate reader (Tecan, Männedorf, Switzerland) after 24 h, 48 h and 96 h of incubation.

Substrate utilization profiles obtained from Biolog™ ECO-plate readouts were analyzed according to Brinkmann et al. (2021), using the rate of substrate utilization measured as the change in observed optical density (OD) between 24 h and 48 h of incubation, which was the measurement interval within which OD showed the steepest change (SI Figure 4). From this, total well-color development (TWCD), average well-color development (AWCD) and measures of α-diversity (substrate utilization richness, Simpson 1-D and Shannon-Weiner index scores) and β-diversity (Bray-Curtis index) were calculated. In addition, TWCD and substrate utilization richness were calculated per substrate group.

2.6. *Ischnura elegans* - in-situ conditions and assessment of endpoints

I. elegans larvae were collected from a pond adjacent to the experimental site using a dipnet (mesh size ϴ 0.5 mm), inspected visually for external damage (presence of all caudal lamellae and appendages), and selected according to body length (11 ± 0.08 mm, mean ± SE, $n = 35$) measured as described for *L. stagnalis*). Prior to the experiment, *I. elegans* larvae were conditioned in water from the experimental site which was filtered from zooplankton (filter mesh size ϴ 53 μm, EFE & GB Nets,

Cornwall, UK) for a period of 14 days, during which they were fed live larvae of *Chironomus sp.* (~2–4 mm, 3rd-4th instar, purchased from a commercial retailer) *ad libitum*. *Chironomus sp.* larvae have previously been shown to constitute a common prey item in the diet of *I. elegans* larvae (Thompson, 1978), and in the current experiment, *I. elegans* larvae were observed to feed readily on provided *Chironomus sp.* larvae during the conditioning phase. *I. elegans* larvae were subsequently inspected visually as previously described, and selected individuals were distributed randomly over 35 cages (one individual per cage) consisting of a stainless steel (mesh size ϴ 1 mm) outer layer and an acrylic inner layer fitted with a ϴ 53 μm mesh (volume of inner cage ~800 mL, SI Figure 1). A piece of PVC-coated steel wire was placed upright in each cage to provide a substrate for *I. elegans* to attach to, and to allow vertical movement towards the water surface in preparation for emergence (see below). Cages were placed on top of the sediment of the mesocosms on the day of treatment application and removed every alternating day to provide five live *Chironomus sp.* larvae as food, and to assess survival, emergence, and number of consumed *Chironomus sp.* larvae. From 25 days after the application of the treatments onwards, emergence of *I. elegans* as imagines (i.e., adults) was facilitated by fixing the cages to rods overhanging the mesocosms, ensuring that cages were halfway submerged (i.e., leaving half of the cage above the water surface). *I. elegans* were monitored until all individuals either emerged, after which they were photographed to determine body size (as described for *L. stagnalis*), or died (i.e., 57 days in total).

2.7. Statistical analyses

All data were analyzed using R version 4.2.1 (R Core Team, 2022) and where applicable, reported *p*-values have been adjusted for multiple testing. Test results were considered statistically significant at $p < 0.05$.

L. stagnalis survival rates were compared between treatments using binomially-distributed generalized mixed-effect models (GLMMs, function 'glmer', R package 'lme4'), in which random intercepts were fitted for data from separate mesocosms to account for the repeated measures design. Convergence issues were mitigated by centering the variable sampling day, and by selection of the optimal model (BOBYQA) optimizer using the 'allFit' function (R package 'afex'). Bonferroni-Holm-corrected estimated marginal means were calculated to compare survival rates between treatments and controls for each sampling day (function 'emmeans', R package 'emmeans').

Differences between treatments in growth (increase in shell length and wet weight from starting conditions) and feeding (decrease in DECOTAB wet weight from starting conditions) of surviving *L. stagnalis* were analyzed using one-way ANOVAs (function 'aov', R package 'stats'), and differences in periphyton development (accumulated dry mass at the end of the experiment) were assessed accordingly. Assumptions of normality of model residuals and homoskedasticity were assessed visually using Q-Q plots and residuals vs. leverage plots. In case assumptions for parametric tests were not met, data were either $\log_{10}(x + 1)$-transformed, box-cox transformed, or analyzed using non-parametric Kruskal-Wallis tests (function 'kruskal.test', R package 'stats'). Where relevant, post-hoc comparisons were performed using Tukey's Honestly Significant Difference (HSD) test, and *p*-values were Tukey-adjusted to account for multiple testing (function 'TukeyHSD', R package 'stats'). Correlations between survival, growth and feeding rates of *L. stagnalis* were assessed via linear regressions (function 'lm', R package 'stats').

Biolog™ ECO-plate TWCD, AWCD and substrate utilization richness (overall and per substrate group) as well as Simpson 1-D and Shannon-Wiener index scores were compared between treatments and controls as described for growth- and feeding of *L. stagnalis*. Dissimilarity in community substrate utilization profiles from Biolog™ ECO-plates between treatments was assessed through permutational analysis of variance (PERMANOVA, function 'adonis2', R package 'vegan') performed on Bray-Curtis dissimilarity indexes. Differences in homogeneity of multivariate dispersions (i.e. β-dispersion) were assessed through a permutation-based test of multivariate homogeneity of group dispersions (function 'permutest', R package 'Vegan').

Survival and emergence data from *I. elegans* were used to fit Cox proportional hazards mixed-effects models (function 'coxme', R package 'coxme'), accounting for the repeated measures design by fitting random intercepts for data from separate mesocosms. Survival probabilities were estimated and compared between treatments by applying right-censoring to data from individuals that emerged as imagines, and emergence probabilities were estimated and compared *vice versa*. Assumptions of proportional hazards were assessed using the 'cox.zph' function (R package 'survival'), and overall treatment effects were assessed by comparing the full model (including treatment) to a null model (excluding treatment).

Feeding rates (measured as the cumulative number of consumed *Chironomus sp.* larvae over time) were compared between treatments using a generalized additive mixed-effects model (GAMMs, function 'gamm', R package 'mgcv'), applying a smoothing term (penalized cubic spline) for time, and accounting for the repeated measures design by fitting random intercepts for data from separate mesocosms. When individuals died or emerged, their data derived from subsequent time-points were excluded from the models to avoid artificial under representations of feeding rates. The total time until emergence, total number of consumed *Chironomus sp.* larvae (i.e., over the course of each individual time in the experiment), mean number of *Chironomus sp.* larvae consumed per day (i.e., normalized for the time each individual spent in the experiment), and body size upon emergence were compared between treatments as described for growth- and feeding of *L. stagnalis*.

3. Results and discussion

3.1. Fate of applied stressors and physicochemical water quality parameters

Time weighted average (TWA) concentrations of $nTiO_2$ measured in the mesocosms were 11.45 ± 1.04 and 8.16 ± 0.29 μg L^{-1} (mean ± SE) for the duration of the *L. stagnalis* and *I. elegans* bioassays, respectively. For the duration of the *L. stagnalis* bioassay, TWA concentrations of carbendazim were 0.41 ± 0.04 μg L^{-1} in carbendazim treatments, 0.48 ± 0.03 μg L^{-1} in carbendazim & $nTiO_2$ treatments, and 0.23 ± 0.02 μg L^{-1} in $nTiO_2$-coated carbendazim treatments (measured as the sum of freely dissolved and $nTiO_2$-coated carbendazim). For the duration of the *I. elegans* bioassay, TWA concentrations of carbendazim were 0.21 ± 0.1 μg L^{-1} in carbendazim treatments, 0.26 ± 0.1 μg L^{-1} in carbendazim & $nTiO_2$ treatments, and 0.12 ± 0.01 μg L^{-1} in $nTiO_2$-coated carbendazim treatments. An overview of measured concentrations of the applied stressors is provided in SI Table 1, and their characterization and fate has been discussed extensively in Nederstigt et al. (2022). Physicochemical water quality parameters showed minimal differences between treatments over the course of both bioassays (SI Table 2).

3.2. Lymnaea stagnalis: survival, growth and feeding

L. stagnalis survival rates declined significantly in response to treatments, with the majority of all mortality occurring within the first 9 days after their application (Treatment - $\chi^2_{(4)} = 10.5$, $p = 0.03$, Time - $\chi^2_{(1)} = 53.7$, $p = 2.3 \times 10^{-13}$, Treatment × Time - $\chi^2_{(4)} = 4.30$, $p = 0.36$, Fig. 1a). Differences in survival rates could predominantly be attributed to $nTiO_2$ and carbendazim & $nTiO_2$ treatments, in which relative reductions from controls of approximately 40 % ($nTiO_2$ - z-value = −2.20, $p = 0.03$) and 50 % (carbendazim & $nTiO_2$ - z-value = −2.98, $p = 2.9 \times 10^{-3}$) were observed (SI Table 3). A less pronounced (~25 %), yet statistically significant overall reduction in survival rates was observed in the $nTiO_2$-coated carbendazim treatments (z-value = −1.97, $p = 0.049$). *L. stagnalis* in treatments in which carbendazim was applied

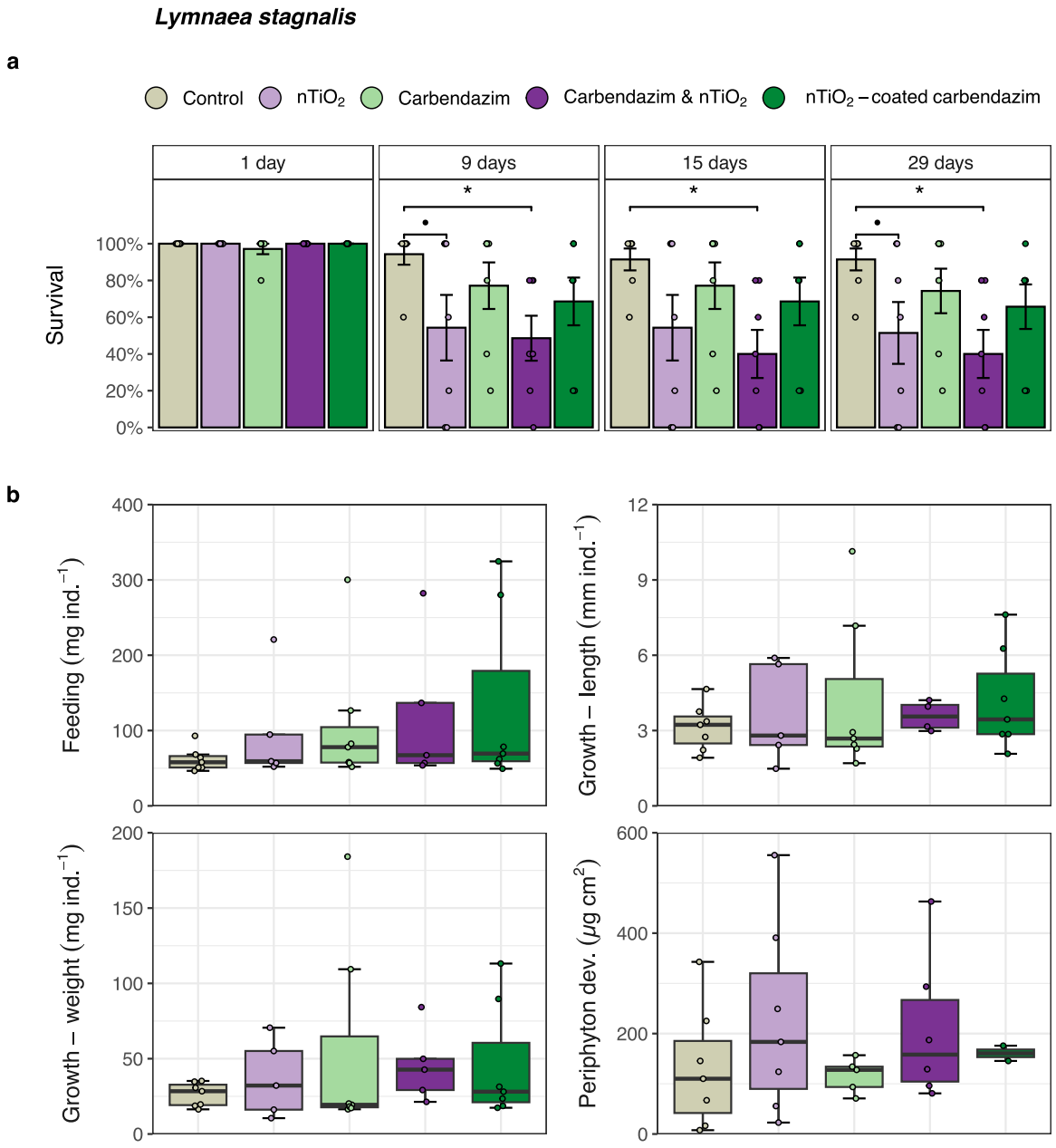

Fig. 1. a. Survival (% of surviving individuals) of *Lymnaea stagnalis* over the course of the bioassay. **b**. Feeding (change in DECOTAB dry weight from starting conditions) and growth (change in shell length and wet weight from starting conditions) of *L. stagnalis* that survived until the end of the bioassay, and periphyton development (accumulated dry mass at the end of the experiment) by the end of the bioassay. For periphyton development, several replicates were excluded from analyses as upon retrieval these proved to have become detached from the construction affixing them upright, leaving part of the surface unexposed to the surrounding water (i.e., two, one, and five replicates in carbendazim, carbendazim & $nTiO_2$ and $nTiO_2$-coated carbendazim treatments, respectively). **a.** Bars indicate means and whiskers indicate standard errors of the mean. **b**. Lines, boxes, and whiskers denote the median, interquartile range, and 1.5 × the interquartile range, respectively. Asterisks indicate statistical significance (. $p = 0.05$, * $p < 0.05$, ** $p < 0.01$, *** $p < 0.001$). See SI Tables 3 & 4 for full output of statistical tests.

in its non-coated form showed the smallest reduction in survival rates (z-value = −1.32, $p = 0.19$), although notably, their survival rates did not differ significantly from those in $nTiO_2$-coated carbendazim treatments (z-value = 0.71, $p = 1.00$).

Feeding ($F_{(4,30)} = 1.91$, $p = 0.13$) and growth (length - $F_{(4,30)} = 0.24$, $p = 0.91$, weight - $\chi^2_{(4)} = 2.18$, $p = 0.70$) of surviving *L. stagnalis* did not differ significantly between treatments over the course of the bioassay (Fig. 1b). Similarly, the total periphyton development over the course of the experiment showed no differences between treatments ($F_{(4,22)} = 0.73$, $p = 0.58$, Fig. 1b). In line with observations from survival rates, both feeding and growth of *L. stagnalis* showed substantially more variation within treatments than within controls. In addition, survival rates were found to be negatively correlated with both feeding and growth of (surviving) *L. stagnalis* (Survival : Feeding - $R^2 = 0.79$, $p < 0.001$, Survival : Length $R^2 = 0.58$, $p < 0.001$, Survival : Weight $R^2 = 0.59$, $p < 0.001$, SI Figure 2). Food consumption of DECOTABs by *L. stagnalis* was found not to interact significantly with treatments in predicting survival (Treatment × Feeding - $\chi^2_{(4)} = 4.9$, $p = 0.30$). This indicates that regardless of treatment, individuals in replicates where survival rates were lower exhibited elevated feeding and growth rates through benefitting from reduced crowding in the bioassay. It is unlikely that in the current experiment, direct competition for resources played a prominent role in this regard, since replicates where feeding was greatest were observed to have consumed only 15 % of the initially

provided mass of feeding substrate. Therefore, the increase in DECOTAB consumption observed in individuals derived from replicates where survival rates were lower is more likely to be attributable to other factors related to crowding, such as preferential energy allocation towards growth instead of reproduction when reared at lower densities (Van der Steen et al., 1968, Koene and Ter Maat, 2004, Dodd et al., 2018). Lastly, the absence of an overall effect of the treatments on feeding, combined with the absence of an interactive effect between feeding and treatments on survival, suggests that compensatory feeding (i.e., to offset toxicant stress) likely did not occur during the bioassay.

Collectively, the results from the *L. stagnalis* bioassay showed no differentiation between impacts from the $nTiO_2$-coated formulation and those of its active substance (i.e., carbendazim). The absence of significant effects of carbendazim on *L. stagnalis* is in concurrence with previous findings from Van den Brink et al. (2000), which demonstrated no significant short or long-term (9 weeks) adverse effects of carbendazim on *L. stagnalis* abundance in mesocosms at concentrations ranging from 3.3 μg L^{-1} to 1000 μg L^{-1}. To our knowledge, there is no other published work which has assessed the toxicity thresholds of carbendazim or other benzimidazole fungicides on *L. stagnalis*.

Regarding $nTiO_2$, the *L. stagnalis* bioassay showed more pronounced effects on survival rates from the material applied in the $nTiO_2$ and carbendazim & $nTiO_2$ treatments, than from the material applied in the $nTiO_2$-coated carbendazim treatments. Although concentrations of $nTiO_2$ were equivalent across these treatments, the former consisted of a mixture of rutile and anatase crystalline forms of $nTiO_2$, while the latter

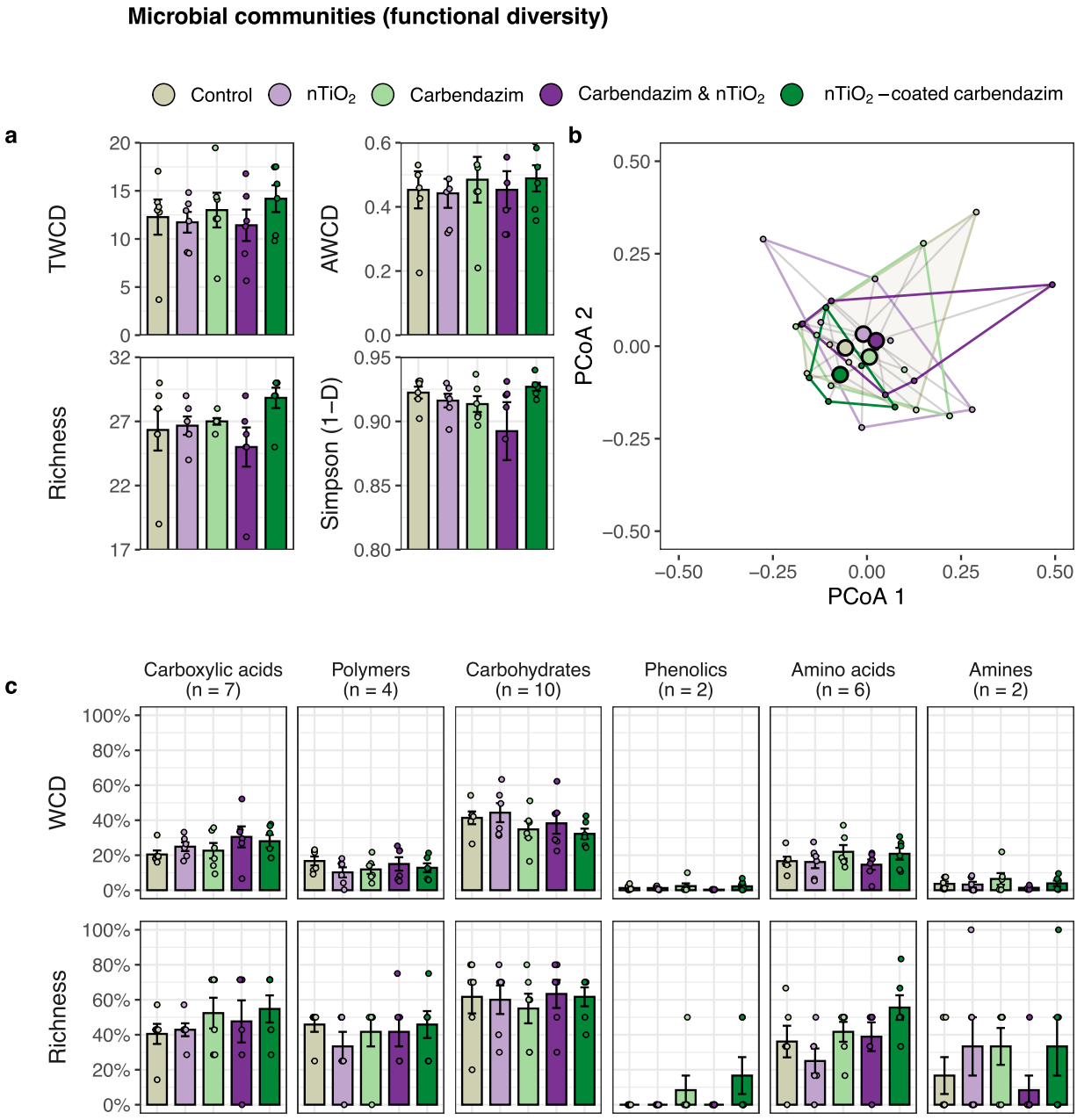

Fig. 2. Functional diversity parameters of DECOTAB-associated microbial communities assessed using Biolog™ ECO-plates. **a.** Total and average well-color development (TWCD and AWCD), substrate utilization richness (calculated from total of 31 substrates) and Simpson diversity (1-D) (mean ± standard error). **b.** Principal coordinate analysis plots (PCoAs, centroids represent mean scores per treatment and polygons are drawn around scores from individual replicates) displaying Bray-Curtis-based functional dissimilarity. **c.** well-color development (WCD) and substrate utilization richness (% of total available substrates, the number of substrates per group are denoted by n) measured per carbon substrate group (mean ± standard error). See SI Table 5 for full output of statistical tests.

exhibited amorphous crystalline structures (see Section 2.2). As stated previously, rutile and anatase $nTiO_2$ act as more effective photocatalysts (i.e., than amorphous structures) when irradiated with UV-A (e.g., by exposure to sunlight), resulting in the generation of higher concentrations of ROS, which under laboratory conditions has been found to be a key contributor to the toxicity of $nTiO_2$ to other freshwater invertebrates through inducing oxidative damage (Bundschuh et al., 2011; Clément et al., 2013; Li et al., 2014; Farner et al., 2019; Coral et al., 2021; Nederstigt et al., 2022). *In-vitro* measurements upon irradiation with UV-A confirmed that the material used in the $nTiO_2$ and carbendazim & $nTiO_2$ treatments exhibits photocatalytic activity through the formation of hydroxyl radicals (•OH), and no photocatalytic activity was observed in the material used in the $nTiO_2$-coated carbendazim treatments (SI Figure 3). Although this provides an indication that ROS production may have contributed to the effects observed in the bioassay with *L. stagnalis*, it should be noted that the observations from our *in-vitro* tests may not be directly applicable to realistic environmental conditions where UV-A can be quenched upon penetration of the water layer, and ROS may readily dissipate by reacting with dissolved and suspended organic matter (Waggoner et al., 2017; Li et al., 2024).

Laboratory-based studies of other aquatic pulmonate snails with grazing-type feeding habits have indicated negative impacts by $nTiO_2$ on endpoints such as fertility in *Physella acuta* (Musee et al., 2010), and oxidative stress-induced cytotoxicity in *Lymnaea luteola* (Ali, 2014 & Ali et al., 2015). Data on the toxicity of $nTiO_2$ in *L. stagnalis* specifically however proves sparse. The findings from the current experiment provide an indication that the contribution of its photocatalytic properties may be a relevant aspect to consider in this regard in future studies.

3.3. Functional diversity of DECOTAB-associated microbial communities

ECO-plate utilization profiles of DECOTAB-associated microbial communities showed no significant differences between treatments and controls in terms of total and average well color development or measures of α-diversity (substrate utilization richness and Simpson 1-D diversity, Shannon-index) when calculated from all (31) available carbon substrates (Fig. 2a, SI Table 5). Likewise, DECOTAB-associated microbial communities did not exhibit significant dissimilarity between treatments and controls in terms of functional (Bray-Curtis-based) β-diversity profiles (PERMANOVA: $F_{(4,25)} = 0.70$, $R^2 = 0.10$, $p = 0.93$, β-dispersion: $F_{(4,25)} = 0.39$, $p = 0.84$, Fig. 2b). When analyzed per substrate group, DECOTAB-associated microbial communities showed more pronounced yet statistically insignificant differences between treatments (Fig. 2c, SI Table 5). Substrates in the carboxylic acids ($n = 7$) and the carbohydrates ($n = 10$) groups showed the highest rates of utilization by microbial communities in terms of WCD and richness. These carbon sources are likely to be more representative of carbon sources commonly utilized by microbial communities in natural environments (Konopka et al., 1998), whereas (insignificant) variability in WCD and richness between treatments for phenolic compounds ($n = 2$) and amines ($n = 2$) may in part be explained by the overall low number of substrates represented and for these substrate groups.

Overall, the findings from the ECO-plate substrate utilization profiles illustrate that DECOTAB-associated microbial communities remained consistent in terms of functional diversity, with no significant loss of functions or shifts in substrate utilization in any of the treatments. It should be noted that due to functional redundancy, measures of functional diversity may be less sensitive to perturbations by stressors than those of taxonomic diversity (Ouwehand et al., 2024). Furthermore, functional diversity (regardless of its means of assessment) may not translate directly to the nutritional quality of microbes present on the feeding substrate of decomposers (Weitere et al., 2018). Nevertheless, the findings from the ECO-plate substrate utilization profiles provide no indication of microbially-mediated indirect effects of the applied treatments on *L. stagnalis*.

3.4. Ischnura elegans: survival, emergence and feeding

Overall survival rates (i.e., successful emergence as imagines) of *I. elegans* over the course of the bioassay were 71 % in controls (5/7 individuals), 86 % (6/7 individuals) in $nTiO_2$ treatments, 57 % (4/7 individuals) in carbendazim treatments, 86 % (6/7 individuals) in carbendazim & $nTiO_2$ treatments, and 71 % (5/7 individuals) in $nTiO_2$-coated carbendazim treatments. Cumulative survival probabilities over the course of the bioassay did not differ significantly between treatments ($\chi^2_{(4)} = 2.20$, $p = 0.70$, Fig. 3a, SI Table 6). Similarly, cumulative emergence probabilities showed minimal differences between treatments ($\chi^2_{(4)} = 2.63$, $p = 0.62$, Fig. 3b, SI Table 6), while surviving *I. elegans* in treatments did show a consistent decrease in the total time until emergence relative to controls ($F_{(4,21)} = 3.07$, $p = 0.04$, Fig. 3d, SI Table 7). This decrease was most pronounced in $nTiO_2$-coated carbendazim treatments (mean difference = −13.6, 95 % CI = −26.4 – −0.8, $p = 0.03$), followed by $nTiO_2$ (mean difference = −11.2, 95 % CI = −23.4 – 1.05, $p = 0.08$), carbendazim (mean difference = −11.5, 95 % CI = −25.0 – 2.0, $p = 0.12$) and carbendazim & $nTiO_2$ (mean difference = −8.8, 95 % CI = −21.1 – 3.4, $p = 0.23$) treatments. Comparisons between individual treatments all yielded p-values > 0.05, and thus provided no indication of significant differences in responses between formulations of carbendazim.

Cumulative feeding rates (until mortality or emergence) of *I. elegans* in treatments showed minimal differences from controls ($F_{(4)} = 0.87$, $p = 0.48$, Fig. 3c, SI Table 7), and this was also reflected in mean feeding rates per day ($F_{(4)} = 0.57$, $p = 0.69$), Fig. 3d, SI Table 8). Consistent with their extended time until emergence however, total feeding rates over the course of the bioassay were higher in controls than in treatments, although differences in this regard were not statistically significant ($F_{(4)} = 1.12$, $p = 0.38$, Fig. 3d, SI Table 7). It should be noted that the endpoints measured in the *I. elegans* bioassay exhibited relatively high variability among replicates, and that the overall mortality rate in the controls exceeded 20 %. Together with a relatively small sample size, these factors are likely to have reduced statistical power in the current experiment. Limitations to this end are more commonly encountered in mesocosm experiments, where natural variability is typically higher than in controlled laboratory settings, and where sample sizes are inherently constrained by logistical factors such as costs and labor intensity (Macaulay et al., 2025). Consequently, the findings presented here are best interpreted as conservative estimates of responses of *I. elegans* to the applied stressors.

Populations of *I. elegans* and other Odonata have been observed to respond to various stressors by both shortening as well as extending their time spent until emergence (Arambourou and Stoks, 2015; Barmentlo et al., 2019; Antoł et al., 2022). Shortening of the time until emergence can serve as a means to reduce time spent in unfavorable conditions as larvae (e.g., to minimize exposure to toxicants, or avoid predation), but can come at a tradeoff with a reduction in adult body size and other energetic parameters upon emergence (Arambourou and Stoks, 2015). In addition to representing a fitness cost for *I. elegans* (e.g., through a subsequent reduction in reproductive- and predatory success), this may also result in emerged adults being of lower nutritional value to predators. In the current study however, body size of successfully emerged individuals was found to vary minimally across treatments, and showed no relationship with cumulative feeding rates across the experimental timeframe ($\chi^2_{(4)} = 0.87$, $p = 0.48$, Fig. 3d). Considering that *I. elegans* is known emerge throughout the season and exhibits a long imago phase (and thus does not rely on strict synchronization of emergence for reproduction), the ecological implications of the slight reduction in emergence time observed in the current experiment, if any, are likely to be minimal.

4. Conclusions

Agricultural applications of nanomaterials present both challenges

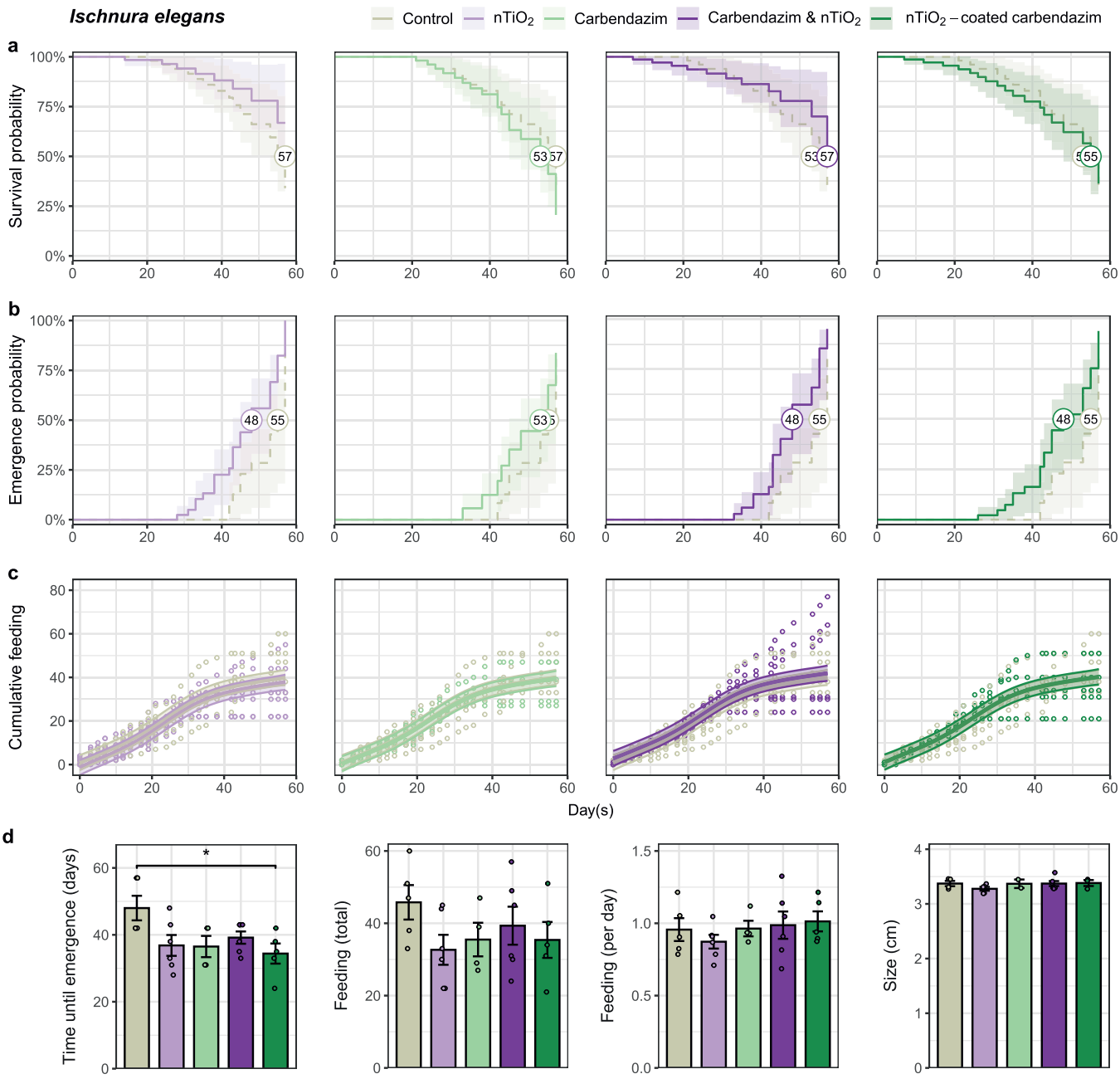

Fig. 3. Survival (**a**) and emergence (**b**) probabilities (prediction ± 95 % confidence intervals) of *Ischnura elegans* across the timeframe of the bioassay derived from time-to-event analyses (accounting for right-censoring of data from individuals after they have either emerged or died). (**c**) Cumulative number of consumed *Chironomus sp.* larvae until mortality or emergence and back-transformed predictions from generalized additive models (predictions ± 95 % confidence intervals). Total time until emergence, total number of consumed *Chironomus sp.* larvae until emergence, number of *Chironomus sp.* larvae consumed per day until emergence, and body size upon emergence (**d**) calculated excluding individuals that died over the course of the bioassay (mean ± standard error). Note that for measures of body size, several individuals were excluded from analyses due to escape upon emergence. For survival and emergence probabilities and cumulative feeding rates, treatments have been contrasted separately with controls to improve readability. Annotated circles (**a** & **b**) denote median survival and emergence times. Asterisks indicate statistical significance (. $p = 0.05$, * $p < 0.05$, ** $p < 0.01$, *** $p < 0.001$). See SI Tables 6, 7, and 8 for full output of statistical tests.

and opportunities with regard to the development of more sustainable agricultural practices. The current study provides no indication of differences between non-target impacts from the applied nano-enabled formulation and those of its active substance. Nevertheless, the observed decrease in survival rates of *L. stagnalis* upon exposure to environmentally realistic concentrations of rutile and anatase $nTiO_2$, in contrast to amorphous $nTiO_2$ (as applied in the $nTiO_2$-coated carbendazim treatments), alerts to the importance of its crystalline structure and photocatalytic activity when evaluating its toxicity. As such, the findings from the current study highlight that for nano-enabled formulations of pesticides, selection of appropriate carrier materials may be an important factor regarding mitigation of non-target impacts. Considering that $nTiO_2$ is currently applied in a wide variety of products, and that its production and emission volumes currently far exceed those of other nanomaterials, the applicability of these findings furthermore spans beyond the potential use of $nTiO_2$ for agricultural purposes.

CRediT authorship contribution statement

Tom A.P. Nederstigt: Writing – review & editing, Writing – original

draft, Visualization, Supervision, Methodology, Investigation, Formal analysis, Data curation, Conceptualization. **Richard K.M. Frische:** Writing – review & editing, Writing – original draft, Visualization, Methodology, Investigation, Formal analysis, Data curation, Conceptualization. **Jesse Ouwehand:** Writing – review & editing, Methodology, Investigation. **Vijver Martina:** Writing – review & editing, Supervision, Funding acquisition.

Declaration of Competing interest

The authors declare that they have no known competing financial interests or personal relationships that could have appeared to influence the work reported in this paper.

Acknowledgments

The facility maintenance & support for the presented work was kindly funded by the Campusregeling province South Holland. We thank the Joint Research Center (JRC) for providing the nTiO_2 used in the experiment, Ruud van Ommen, Damiano La Zara, Yuyang Tian for preparing, characterizing and providing the nTiO_2-coated carbendazim, Joris Koene for providing the initial batch of *Lymnaea stagnalis* used to start cultures, and Willie Peijnenburg for his contributions to discussions regarding the experimental setup. We express our gratitude to Bob Bastiaans for performing the *Ischnura elegans* assays, and Bo Bode and Mitchel van 't Riet for their overall assistance over the course of the experiments and during subsequent analyses. We also are grateful to all volunteers, employees and students who assisted in the practical work. Tom Nederstigt, Jesse Ouwehand and Martina Vijver are supported by the ERC-consolidator grant granted to Martina Vijver entitled EcoWizard (101002123).

Appendix A. Supporting information

Supplementary data associated with this article can be found in the online version at doi:10.1016/j.ecoenv.2025.118809.

Data availability

Data will be made available on request.

References

Abdel-Latif, H.M.R., Dawood, M.A.O., Menanteau-Ledouble, S., El-Matbouli, M., 2020. Environmental transformation of n-TiO_2 in the aquatic systems and their ecotoxicity in bivalve mollusks: a systematic review. Ecotoxicol. Environ. Saf. 200, 110776. https://doi.org/10.1016/J.ECOENV.2020.110776.

Adam, V., Wu, Q., Nowack, B., 2021. Integrated dynamic probabilistic material flow analysis of engineered materials in all european countries. NanoImpact 22, 100312. https://doi.org/10.1016/j.impact.2021.100312.

Alejandro, M.N.M., Guadalupe, B.E., Omar, T.S.F., Patricia, R.R., 2022. Temporal and spatial analysis of benomyl/carbendazim in water and its possible impact on Nile tilapia (Oreochromis niloticus) from tenango dam, puebla, Mexico. Environ. Monit. Assess. 194 (1), 1–13. https://doi.org/10.1007/S10661-021-09661-3.

Ali, D., 2014. Evaluation of environmental stress by comet assay on freshwater snail *lymnea luteola l.* Exposed to titanium dioxide nanoparticles. Toxicol. Environ. Chem. 96 (8), 1185–1194. https://doi.org/10.1080/02772248.2015.1014195.

Ali, D., Ali, H., Alarifi, S., Kumar, S., Serajuddin, M., Mashih, A.P., Ahmed, M., Khan, M., Adil, S.F., Shaik, M.R., Ansari, A.A., 2015. Impairment of DNA in a freshwater gastropod (*lymnea luteola l.*) after exposure to titanium dioxide nanoparticles. Arch. Environ. Contam. Toxicol. 68 (3), 543–552. https://doi.org/10.1007/S00244-015-0132-0.

Antoł, A., Labecka, A.M., Ronny Larsson, J.I., Sniegula, S., 2022. First record of microsporidia infection in the damselfly *ischnura elegans* larvae: temperature and predator cue effects on the Host's life history. Diversity 14 (6), 428. https://doi.org/10.3390/D14060428.

Arambourou, H., Stoks, R., 2015. Combined effects of larval exposure to a heat wave and chlorpyrifos in Northern and Southern populations of the damselfly *ischnura elegans*. Chemosphere 128, 148–154. https://doi.org/10.1016/J.CHEMOSPHERE.2015.01.044.

Barmentlo, S.H., Vriend, L.M., van Grunsven, R.H.A., Vijver, M.G., 2019. Environmental levels of neonicotinoids reduce prey consumption, mobility and emergence of the damselfly *ischnura elegans*. J. Appl. Ecol. 56 (8), 2034–2044. https://doi.org/10.1111/1365-2664.13459.

Brinkmann, B.W., Beijk, W.F., Vlieg, R.C., van Noort, S.J.T., Mejia, J., Colaux, J.L., Lucas, S., Lamers, G., Peijnenburg, W.J.G.M., Vijver, M.G., 2021. Adsorption of titanium dioxide nanoparticles onto zebrafish eggs affects colonizing microbiota. Aquat. Toxicol. 232, 105744. https://doi.org/10.1016/J.AQUATOX.2021.105744.

Brinkmann, B.W., Koch, B.E.V., Spaink, H.P., Peijnenburg, W.J.G.M., Vijver, M.G., 2020. Colonizing microbiota protect zebrafish larvae against silver nanoparticle toxicity. Nanotoxicology 14 (6), 725–739. https://doi.org/10.1080/17435390.2020.1755469.

Bundschuh, M., Zubrod, J.P., Englert, D., Seitz, F., Rosenfeldt, R.R., Schulz, R., 2011. Effects of nano-TiO_2 in combination with ambient UV-irradiation on a leaf shredding amphipod. Chemosphere 85 (10), 1563–1567. https://doi.org/10.1016/j.chemosphere.2011.07.060.

Clément, L., Hurel, C., Marmier, N., 2013. Toxicity of TiO_2 nanoparticles to cladocerans, algae, rotifers and plants – effects of size and crystalline structure. Chemosphere 90 (3), 1083–1090. https://doi.org/10.1016/J.CHEMOSPHERE.2012.09.013.

Coral, J.A., Kitchens, C.L., Brumaghim, J.L., Klaine, S.J., 2021. Correlating quantitative measurements of radical production by photocatalytic TiO_2 with *daphnia magna* toxicity. Environ. Toxicol. Chem. 40 (5), 1322–1334. https://doi.org/10.1002/ETC.4982.

Dodd, S., Rothwell, C.M., Lukowiak, K., 2018. Strain-specific effects of crowding on long-term memory formation in lymnaea. Comp. Biochem. Physiol. Part A Mol. Integr. Physiol. 222, 43–51. https://doi.org/10.1016/j.cbpa.2018.04.010.

Dudley, N., Alexander, S., 2017. Agriculture and biodiversity: a review. Biodiversity 18 (2–3), 45–49. https://doi.org/10.1080/14888386.2017.1351892.

Eremia, S.A.V., Chevalier-Lucia, D., Radu, G.L., Marty, J.L., 2008. Optimization of hydroxyl radical formation using TiO_2 as photocatalyst by response surface methodology. Talanta 77 (2), 858–862. https://doi.org/10.1016/J.TALANTA.2008.07.056.

Farner, J.M., Cheong, R.S., Mahé, E., Anand, H., Tufenkji, N., 2019. Comparing TiO_2 nanoparticle formulations: stability and photoreactivity are key factors in acute toxicity to: *daphnia magna*. Environ. Sci. Nano 6 (8), 2532–2543. https://doi.org/10.1039/c9en00666d.

Fleeger, J.W., Carman, K.R., Nisbet, R.M., 2003. Indirect effects of contaminants in aquatic ecosystems. Sci. Total Environ. 317 (1–3), 207–233. https://doi.org/10.1016/S0048-9697(03)00141-4.

Flores, L., Banjac, Z., Farré, M., Larrañaga, A., Mas-Martí, E., Muñoz, I., Barceló, D., Elosegi, A., 2014. Effects of a fungicide (imazalil) and an insecticide (diazinon) on stream fungi and invertebrates associated with litter breakdown. *477* Sci. Total Environ. 476, 532–541. https://doi.org/10.1016/J.SCITOTENV.2014.01.059.

Gessner, M.O., Chauvet, E., Dobson, M., 1999. A perspective on leaf litter breakdown in streams. Oikos 85 (2), 377. https://doi.org/10.2307/3546505.

Gligorovski, S., Strekowski, R., Barbati, S., Vione, D., 2015. Environmental implications of hydroxyl radicals (•OH). Chem. Rev. 115 (24), 13051–13092. https://doi.org/10.1021/CR500310B.

Graça, M.A.S., 2001. The role of invertebrates on leaf litter decomposition in streams - a review. Int. Rev. Hydrobiol. 86 (4–5), 383–393. https://doi.org/10.1002/1522-2632(200107)86:4/5<383::AID-IROH383>3.0.CO;2-D.

Grillo, R., Fraceto, L.F., Amorim, M.J.B., Scott-Fordsmand, J.J., Schoonjans, R., Chaudhry, Q., 2021. Ecotoxicological and regulatory aspects of environmental sustainability of nanopesticides (Elsevier B.V). J. Hazard. Mater. 404, 124148. https://doi.org/10.1016/j.jhazmat.2020.124148.

Haase, Bowler, P., Baker, D.E., Bonada, N.J., Domisch, N., Garcia Marquez, S., et al., 2023. The recovery of european freshwater biodiversity has come to a halt. *7974*, *620* Nature 620 (7974), 582–588. https://doi.org/10.1038/s41586-023-06400-1.

Hayles, J., Johnson, L., Worthley, C., Losic, D., 2017. Nanopesticides: a review of current research and perspectives. New Pesticides and Soil Sensors. Elsevier, pp. 193–225. https://doi.org/10.1016/b978-0-12-804299-1.00006-0.

Hendricks, N., Olatunji, O., Ofori, I., Gumbi, B.P., 2023. Occurrence, fate, and impact of engineered metal/carbonaceous nanomaterials in the environment, detection, and quantitation methods. Int. J. Environ. Sci. Technol. 20 (11), 12937–12954. https://doi.org/10.1007/S13762-023-04977-8.

Hieber, M., Gessner, M.O., 2002. Contribution of stream detrivores, fungi, and bacteria to leaf breakdown based on biomass estimates. Ecology 83 (4), 1026. https://doi.org/10.2307/3071911.

Hitt, N.P., Bonneau, L.K., Jayachandran, K.V., Marchetti, M.P., 2015. Freshwater ecosystems and biodiversity. Lessons Conserv. 5, 15–16. ⟨ncep.amnh.org/linc/⟩.

Hofmann, T., Lowry, G.V., Ghoshal, S., Tufenkji, N., Brambilla, D., Dutcher, J.R., Gilbertson, L.M., Giraldo, J.P., Kinsella, J.M., Landry, M.P., Lovell, W., Naccache, R., Paret, M., Pedersen, J.A., Unrine, J.M., White, J.C., Wilkinson, K.J., 2020. Technology readiness and overcoming barriers to sustainably implement nanotechnology-enabled plant agriculture. In: Nature Food, 1. Nature Publishing Group, pp. 416–425. https://doi.org/10.1038/s43016-020-0110-1.

Kah, M., Sabliov, C., Wang, Y., White, J.C., 2023. Nanotechnology as a foundational tool to combat global food insecurity. In: In One Earth, 6. Cell Press, pp. 772–775. https://doi.org/10.1016/j.oneear.2023.06.011.

Kampfraath, A.A., Hunting, E.R., Mulder, C., Breure, A.M., Gessner, M.O., Kraak, M.H.S., Admiraal, W., 2012. DECOTAB: a multipurpose standard substrate to assess effects of litter quality on microbial decomposition and invertebrate consumption. Freshw. Sci. 31 (4), 1156–1162. https://doi.org/10.1899/12-075.1.

Keller, A.A., Ehrens, A., Zheng, Y., Nowack, B., 2023. Developing trends in nanomaterials and their environmental implications. Nat. Nanotechnol. 18 (8), 834–837. https://doi.org/10.1038/s41565-023-01409-z.

Koene, J.M., Ter Maat, A., 2004. Energy budgets in the simultaneously hermaphroditic pond snail, *lymnaea stagnalis*: a trade-off between growth and reproduction during development. Belg. J. Zool. 134 (2/1), 41–46.

Koli, P., Singh, B.B., Shakil, N.A., Kumar, J., Kamil, D., 2015. Development of controlled release nanoformulations of carbendazim employing amphiphilic polymers and their bioefficacy evaluation against *rhizoctonia solani*. J. Environ. Sci. Health Part B Pestic. Food Contam. Agric. Wastes 50 (9), 674–681. https://doi.org/10.1080/03601234.2015.1038961.

Konopka, A., Oliver, L., Turco, R.F., 1998. The use of carbon substrate utilization patterns in environmental and ecological microbiology. Microb. Ecol. 35 (2), 103–115. https://doi.org/10.1007/S002489900065.

Kookana, R.S., Boxall, A.B.A., Reeves, P.T., Ashauer, R., Beulke, S., Chaudhry, Q., Cornelis, G., Fernandes, T.F., Gan, J., Kah, M., Lynch, I., Ranville, J., Sinclair, C., Spurgeon, D., Tiede, K., Van Den Brink, P.J., 2014. Nanopesticides: guiding principles for regulatory evaluation of environmental risks. J. Agric. Food Chem. 62 (19), 4227–4240. https://doi.org/10.1021/jf500232f.

Kumar, S., Kumar, D., Dilbaghi, N., 2017. Preparation, characterization, and bio-efficacy evaluation of controlled release carbendazim-loaded polymeric nanoparticles. Environ. Sci. Pollut. Res. 24 (1), 926–937. https://doi.org/10.1007/s11356-016-7774-y.

Li, S., Wallis, L.K., Ma, H., Diamond, S.A., 2014. Phototoxicity of TiO_2 nanoparticles to a freshwater benthic amphipod: are benthic systems at risk? Sci. Total Environ. 466, 800–808. https://doi.org/10.1016/j.scitotenv.2013.07.059.

Li, B., Wang, S., Fessler, M., Zou, R., Su, Y., Zhang, Y., 2024. Differential interactions between natural clay minerals and dissolved organic matter affect reactive oxygen species formation. Water Res. 249, 120984. https://doi.org/10.1016/J.WATRES.2023.120984.

Macaulay, S.J., Jeppesen, E., Riebesell, U., Nejstgaard, J.C., Berger, S.A., Lewandowska, A.M., Rico, A., Kefford, B.J., Vad, C.F., Costello, D.M., et al., 2025. Addressing grand ecological challenges in aquatic ecosystems: how can mesocosms be used to advance solutions? Oikos, e11020. https://doi.org/10.1111/oik.11020.

Merel, S., Benzing, S., Gleiser, C., Di Napoli-Davis, G., Zwiener, C., 2018. Occurrence and overlooked sources of the biocide carbendazim in wastewater and surface water. Environ. Pollut. 239, 512–521. https://doi.org/10.1016/J.ENVPOL.2018.04.040.

Mohan, A., Matthews, B., Räsänen, K., 2024. Direct and indirect effects of chemical pollution: fungicides alter growth, feeding, and pigmentation of the freshwater detritivore asellus aquaticus. Ecotoxicol. Environ. Saf. 285, 117017. https://doi.org/10.1016/J.ECOENV.2024.117017.

Musee, N., Oberholster, P.J., Sikhwivhilu, L., Botha, A.M., 2010. The effects of engineered nanoparticles on survival, reproduction, and behaviour of freshwater snail, *physa acuta* (Draparnaud, 1805). Chemosphere 81 (10), 1196–1203. https://doi.org/10.1016/j.chemosphere.2010.09.040.

Nabi, M.M., Wang, J., Goharian, E., Baalousha, M., 2022. Temporal variation in TiO_2 engineered particle concentrations in the broad river during dry and wet weathers. Sci. Total Environ. 807, 151081. https://doi.org/10.1016/J.SCITOTENV.2021.151081.

Nederstigt, T.A.P., Brinkmann, B.W., Peijnenburg, W.J.G.M., Vijver, M.G., 2024. Sustainability claims of nanoenabled pesticides require a more thorough evaluation. Environ. Sci. Technol. 58 (5), 2163–2165. https://doi.org/10.1021/ACS.EST.3C10207.

Nederstigt, T.A.P., Peijnenburg, W.J.G.M., Bleeker, E.A., Vijver, M.G., 2022. Applicability of nanomaterial-specific guidelines within long-term *daphnia magna* toxicity assays: a case study on multigenerational effects of $nTiO_2$ and $nCeO_2$ exposure in the presence of artificial daylight. Regul. Toxicol. Pharmacol. 131, 105156. https://doi.org/10.1016/j.yrtph.2022.105156.

Nederstigt, T.A.P., Peijnenburg, W.J.G.M., Schrama, M., van Ommen, J.R., Vijver, M.G., 2022. Impacts of a novel controlled-release TiO_2-coated (nano-)formulation of carbendazim and its constituents on freshwater macroinvertebrate communities. Sci. Total Environ. 838, 156554. https://doi.org/10.1016/j.scitotenv.2022.156554.

OECD. 2004.Test No. 202: Daphnia sp. Acute Immobilisation Test. OECD Guideline for the Testing of Chemicals, Section 2, April. https://doi.org/10.1787/9789264069947-EN.

Ouwehand, J., Peijnenburg, W.J.G.M., Vijver, M.G., 2024. Microbial function matters: Microbiome-aware nano-ecotoxicology needs functional endpoints besides compositional data. Chemosphere 369, 143905. https://doi.org/10.1016/J.CHEMOSPHERE.2024.143905.

Peters, R.J.B., van Bemmel, G., Milani, N.B.L., den Hertog, G.C.T., Undas, A.K., van der Lee, M., Bouwmeester, H., 2018. Detection of nanoparticles in Dutch surface waters. Sci. Total Environ. 621, 210–218. https://doi.org/10.1016/J.SCITOTENV.2017.11.238.

Pietz, S., Kolbenschlag, S., Röder, N., Roodt, A.P., Steinmetz, Z., Manfrin, A., Schwenk, K., Schulz, R., Schäfer, R.B., Zubrod, J.P., Bundschuh, M., 2023. Subsidy quality affects common riparian Web-Building spiders: consequences of aquatic contamination and food resource. Environ. Toxicol. Chem. 42 (6), 1346–1358. https://doi.org/10.1002/ETC.5614.

R Core Team, 2022. R: a language and environment for statistical computing. (4.2.1). R. Found. Stat. Comput. ⟨https://www.r-project.org/⟩.

Reid, A.J., Carlson, A.K., Creed, I.F., Eliason, E.J., Gell, P.A., Johnson, P.T.J., Kidd, K.A., MacCormack, T.J., Olden, J.D., Ormerod, S.J., Smol, J.P., Taylor, W.W., Tockner, K., Vermaire, J.C., Dudgeon, D., Cooke, S.J., 2019. Emerging threats and persistent conservation challenges for freshwater biodiversity. Biol. Rev. 94 (3), 849–873. https://doi.org/10.1111/BRV.12480.

Sánchez-Bayo, F., Ortiz-Santaliestra, M.E., 2021. Indirect effect of pesticides on insects and other arthropods. Toxics 9, 177. https://doi.org/10.3390/TOXICS9080177.

Schäfer, R.B., van den Brink, P.J., Liess, M., 2011. Impacts of pesticides on freshwater ecosystems. Ecological Impacts of Toxic Chemicals. Bentham Science Publisher, pp. 111–137. https://doi.org/10.2174/978160805121211101010111.

Schaller, J., Brackhage, C., 2015. Invertebrate grazers affect metal/metalloid fixation during litter decomposition. Chemosphere 119, 394–399. https://doi.org/10.1016/J.CHEMOSPHERE.2014.07.002.

Schneider, C.A., Rasband, W.S., Eliceiri, K.W., 2012. NIH image to ImageJ: 25 years of image analysis, 1.53a Nat. Methods 9 (7), 671–675. https://doi.org/10.1038/nmeth.2089.

Schulz, R., Bundschuh, M., Entling, M.H., Jungkunst, H.F., Lorke, A., Schwenk, K., Schäfer, R.B., 2024. A synthesis of anthropogenic stress effects on emergence-mediated aquatic-terrestrial linkages and riparian food webs. Sci. Total Environ. 908, 168186. https://doi.org/10.1016/J.SCITOTENV.2023.168186.

Schwarzenbach, R.P., Escher, B.I., Fenner, K., Hofstetter, T.B., Johnson, C.A., Von Gunten, U., Wehrli, B., 2006. The challenge of micropollutants in aquatic systems. Science 313 (5790), 1072–1077. https://doi.org/10.1126/SCIENCE.1127291.

Steen, W.J. Van Der, Jager, J.C., Hoven, N.P. Van Den, 1968. A method for breeding and studying freshwater snails under continuous water change, with some remarks on growth and reproduction in *lymnaea stagnalis* (L.). Neth. J. Zool. 19 (1), 131–139. https://doi.org/10.1163/002829669X00170.

Thompson, D.J., 1978. Prey size selection by larvae of the damselfly, *ischnura elegans* (Odonata). J. Anim. Ecol. 47 (3), 769–785. https://doi.org/10.2307/3670.

Van den Brink, Hattink, J., Bransen, F., Van Donk, E., Brock, T.C., 2000. Impact of the fungicide carbendazim in freshwater microcosms. II. Zooplankton, primary producers and final conclusions. Aquat. Toxicol. 48 (2–3), 251–264. https://doi.org/10.1016/S0166-445X(99)00037-5.

Waggoner, D.C., Wozniak, A.S., Cory, R.M., Hatcher, P.G., 2017. The role of reactive oxygen species in the degradation of lignin derived dissolved organic matter. Geochim. Cosmochim. Acta 208, 171–184. https://doi.org/10.1016/J.GCA.2017.03.036.

Wan, N.-F., Fu, L., Dainese, M., Kiær, L.P., Hu, Y.-Q., Xin, F., Goulson, D., Woodcock, B. A., Vanbergen, A.J., Spurgeon, D.J., Shen, S., Scherber, C., 2025. Pesticides have negative effects on non-target organisms. *2025 16:1* Nat. Commun. 16 (1), 1–16. https://doi.org/10.1038/s41467-025-56732-x.

Wan, Y., Tran, T.M., Nguyen, V.T., Wang, A., Wang, J., Kannan, K., 2021. Neonicotinoids, fipronil, chlorpyrifos, carbendazim, chlorotriazines, chlorophenoxy herbicides, bentazon, and selected pesticide transformation products in surface water and drinking water from Northern Vietnam. Sci. Total Environ. 750, 141507. https://doi.org/10.1016/J.SCITOTENV.2020.141507.

Wang, D., Saleh, N.B., Byro, A., Zepp, R., Sahle-Demessie, E., Luxton, T.P., Ho, K.T., Burgess, R.M., Flury, M., White, J.C., Su, C., 2022. Nano-enabled pesticides for sustainable agriculture and global food security. *2022 17:4* Nat. Nanotechnol. 17 (4), 347–360. https://doi.org/10.1038/s41565-022-01082-8.

Weitere, M., Erken, M., Majdi, N., Arndt, H., Norf, H., Reinshagen, M., Traunspurger, W., Walterscheid, A., Wey, J.K., 2018. The food web perspective on aquatic biofilms. Ecol. Monogr. 88 (4), 543–559. https://doi.org/10.1002/ecm.1315.

Zhai, Y., Brun, N.R., Bundschuh, M., Schrama, M., Hin, E., Vijver, M.G., Hunting, E.R., 2018. Microbially-mediated indirect effects of silver nanoparticles on aquatic invertebrates. Aquat. Sci. 80 (4), 44. https://doi.org/10.1007/s00027-018-0594-z.

Zhang, Y., Goss, G.G., 2022. Nanotechnology in agriculture: comparison of the toxicity between conventional and nano-based agrochemicals on non-target aquatic species. J. Hazard. Mater. 439, 129559. https://doi.org/10.1016/J.JHAZMAT.2022.129559.

Zubrod, J.P., Bundschuh, M., Feckler, A., Englert, D., Schulz, R., 2011. Ecotoxicological impact of the fungicide tebuconazole on an aquatic decomposer-detritivore system. Environ. Toxicol. Chem. 30 (12), 2718–2724. https://doi.org/10.1002/ETC.679.